Canadian Mineralogist
Vol. 21, pp. 517-528 (1983)

GRUNERITE FROM THE SHINYAMA ORE DEPOSIT, KAMAISHI MINE, JAPAN

ETSUO UCHIDA*

Geological Institute, Faculty of Science, University of Tokyo, 7-3-1 Hongo, Bunkyo-ku, Tokyo 113, Japan

Abstract

Most of the clinopyroxene in the clinopyroxene skarn that contains the 4D copper orebody of the Shinyama ore deposit (Japan) was altered to amphibole owing to late-stage decrease of temperature. Two amphibole species are found: Ca-amphibole and cummingtonite–grunerite; the latter is rarely found in skarn-type ore deposits. In exoskarns derived from limestone, the following zonal arrangement is observed from the limestone to the igneous rock: cummingtonite–grunerite skarn, Ca-amphibole skarn, (clinopyroxene skarn) and garnet skarn. This arrangement is attributable to the increase in the chemical potential of CO_2 toward the limestone.

Keywords: cummingtonite–grunerite, Kamaishi mine, Shinyama deposit, skarn, zonal arrangement, phase equilibria, thermochemical data, $X(CO_2)$, Japan.

Sommaire

Le gîte 4D du gisement cuprifère de Shinyama (Japon) se présente dans un skarn à clinopyroxène. Ce pyroxène s'est en grande partie altéré en amphibole à la suite d'une baisse tardive de la température. Deux espèces d'amphibole sont représentées: l'une, amphibole calcique et l'autre, membre de la série cummingtonite–grunérite, rarement trouvée dans les gisements de type skarn. Dans les exoskarns dérivés de calcaire, on observe les zones suivantes, du calcaire vers la roche ignée: skarn à cummingtonite–grunérite, skarn à amphibole calcique, (skarn à clinopyroxène) et skarn à grenat. On peut attribuer cette disposition en zones à l'augmentation du potentiel chimique du CO_2 en direction du calcaire.

(Traduit par la Rédaction)

Mots-clés: cummingtonite–grunérite, mine de Kamaishi, gisement de Shinyama, skarn, distribution en zones, équilibre de phases, données thermochimiques, $X(CO_2)$, Japon.

Introduction

Clinopyroxene skarn of the 4D copper orebody of the Shinyama deposit of the Kamaishi mine underwent strong late-stage alteration. Most of the clinopyroxene in the skarn was altered to amphibole, previously considered to be Ca-amphibole (actinolite to common hornblende). The present study, based on compositions of amphibole determined by the electron-probe microanalyzer, reveals that most are, in fact, cummingtonite–grunerite containing only a small calcium component. Grunerite is common in metamorphosed iron-formations (*cf.* Mueller 1960), and cummingtonite is widespread in metabasic rocks in the amphibolite facies. But cummingtonite–grunerite is rare in skarn-type ore deposits. In this paper, the amphiboles occurring in skarns around the 4D orebody of the Shinyama deposit are described, and their thermochemical conditions of formation are elucidated.

Geology of The Kamaishi Mining District and Description of the Deposits

The Kamaishi mine, located in the eastern margin of Kitakami massif, is typical of iron–copper skarn-type deposits in Japan. The mine is located near the Hayachine–Goyozan tectonic zone. Mesozoic to Paleozoic sedimentary formations and igneous rocks are distributed around the mining district. The ore deposits of the Kamaishi mine occur near the boundary between the Nagaiwa–Onimaru limestone which is of Carboniferous age and the Ganidake igneous complex of Early Cretaceous age. The limestone is the host rock of the skarns. The Shinyama ore deposit is located on the west side of the Ganidake igneous complex and is the largest in the Kamaishi mining district. It is composed of thirteen orebodies which may be subdivided into three types: iron, copper and iron–copper. The skarn can be roughly divided into clinopyroxene skarn and garnet skarn; the former contains copper orebodies and the latter iron or iron–copper orebodies. Grunerite occurs in clinopyroxene skarn, which encloses the largest copper orebody, called 4D, in the Shinyama ore deposit. The reader will find a more detailed description of the Kamaishi mining district in Hamabe & Yano (1976).

The Skarns Around the 4D and 7D Orebodies

The skarns around the 4D copper and 7D iron–copper orebodies of the Shinyama ore deposit have been described in detail by Uchida & Iiyama (1982); only a summary is given here.

The skarns are formed along the boundary between limestone and diorite to diorite porphyry belonging to the Ganidake igneous complex (Fig. 1).

*Present address: Laboratoire de Minéralogie et Géologie Appliquée, Université Catholique de Louvain, 1348 Louvain-la-Neuve, Belgique.

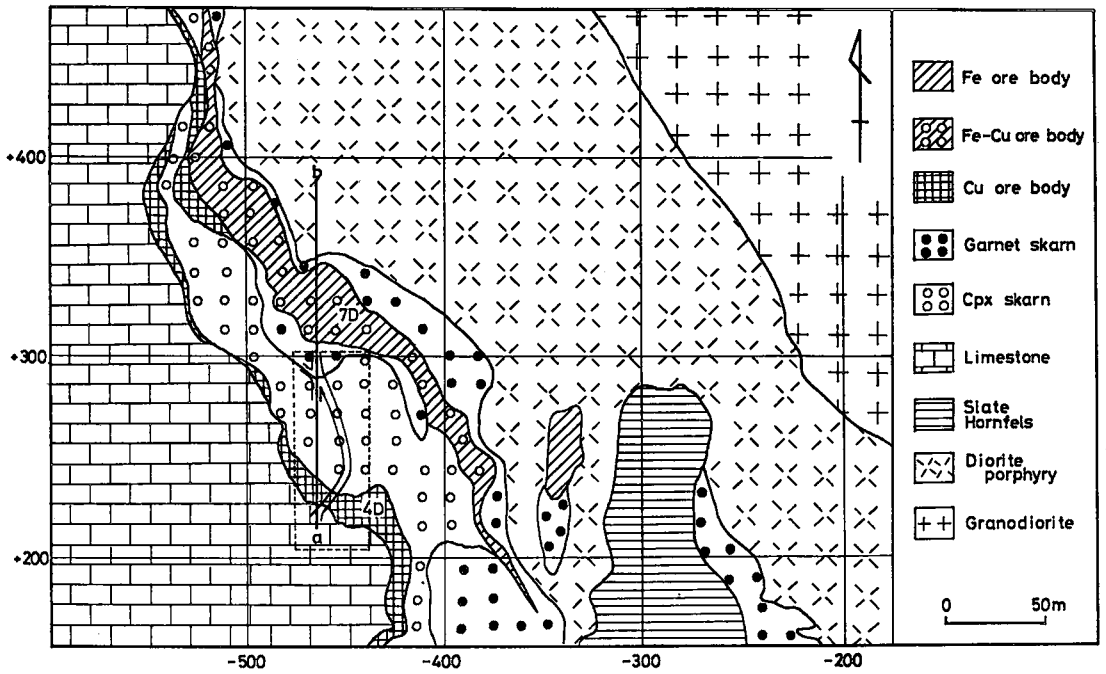

FIG. 1. Geologic plan at the 500-metre level in the vicinity of the Shinyama 4D copper and 7D iron-copper orebodies (after the Kamaishi Mining Company, Ltd.).

They show the following arrangement of zones crossed perpendicular to the boundary, from the limestone toward the igneous rock: clinopyroxene skarn (that encloses the 4D copper orebody), garnet skarn, the 7D iron-copper orebody, garnet-clinopyroxene skarn, epidote-clinopyroxene skarn, epidote-amphibole skarn and plagioclase-amphibole skarn. The latter three are not well developed, compared with the former.

Clinopyroxene skarn is well developed in the upper levels and narrows abruptly toward the lower levels. Most of the clinopyroxene is strongly altered to amphibole and is, at present, rarely found. Garnet skarn, located on the limestone side of the 7D iron-copper orebody, consists mainly of coarse-grained anisotropic garnet with a moderate amount of clinopyroxene. Garnet-clinopyroxene skarn, located on the igneous rock side of the 7D iron-copper orebody, is composed mainly of isotropic to slightly anisotropic garnet and clinopyroxene. Clinopyroxene in garnet and garnet-clinopyroxene skarns is not so strongly altered to amphibole. Judging from the TiO_2 content, and from the size and form of the garnet crystals, garnet skarn is considered to be derived from limestone, and garnet-clinopyroxene skarns from diorite to diorite porphyry (*cf.* Uchida & Iiyama 1982). A network of anisotropic garnet is formed locally along fractures in clinopyroxene skarn; the garnet is similar to that composing the garnet skarn.

OCCURRENCE AND DISTRIBUTION OF AMPHIBOLE

Amphibole occurs in all skarn zones, but is especially abundant in clinopyroxene skarn, garnet skarn, the iron-copper orebody, epidote-amphibole skarn and plagioclase-amphibole skarn. Amphibole in the former three skarns is considered to be an alteration product of clinopyroxene, and that in the latter two skarns is considered to be derived from diorite to diorite porphyry. Amphibolitization of clinopyroxene is weak in garnet-clinopyroxene and epidote-clinopyroxene skarns.

The presence of relict clinopyroxene and of Ca-amphibole pseudomorphs after clinopyroxene (Fig. 3B, D) shows that clinopyroxene skarn was once composed mainly of clinopyroxene. This skarn is, at present, composed mainly of amphiboles, calcite and quartz. Clinopyroxene is observed locally near the networks of anisotropic garnet. Such strong amphibolitization is a typical feature of the 4D copper orebody and is not observed in the other copper orebodies (2D, 3D, 5D and 8D) of the deposit.

Three types of amphibole, cummingtonite-grunerite, actinolite and hornblende, are identified in the clinopyroxene skarn. The following regularity of distribution is recognized for these amphiboles; because it is not very easy to distinguish some Mg-poor actinolite from common hornblende, these two amphiboles are called Ca-amphibole for conve-

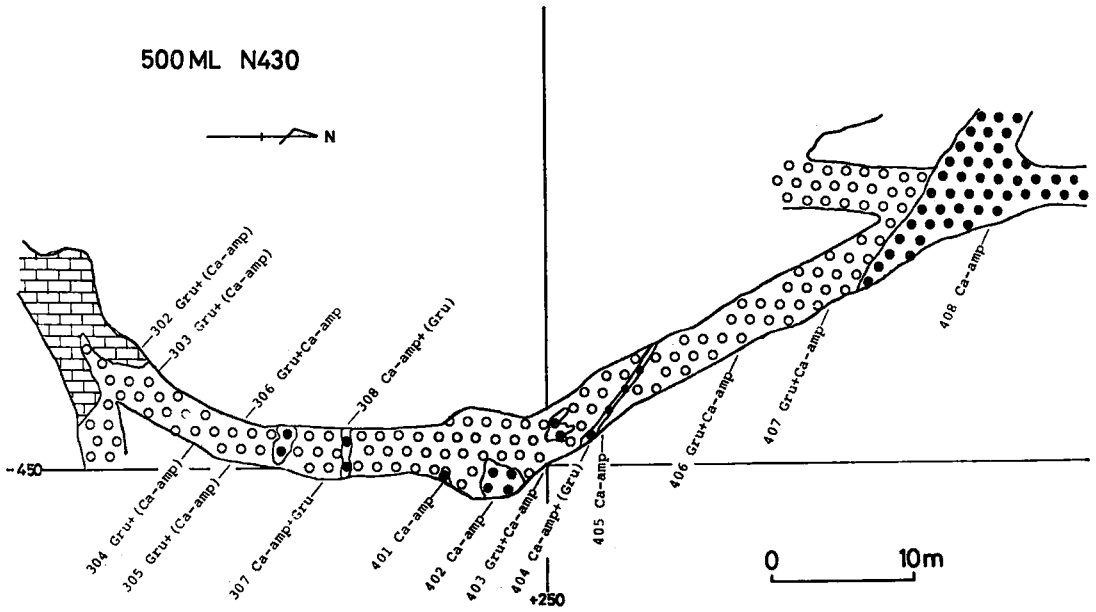

FIG. 2. Distribution of amphiboles in clinopyroxene skarn near N430 of the 500-metre level of the Shinyama ore deposit. This area corresponds to that surrounded by dotted lines in Figure 1. Parentheses indicate a small quantity. Numbers are sample numbers. Legend: see Figure 1.

nience. Figure 2 shows the distribution of these amphiboles in the clinopyroxene skarn near N430 of the 500-metre level. Many garnet networks are observed here (Fig. 3A). There is a tendency for Ca-amphibole to dominate where garnet networks occur, whereas cummingtonite–grunerite dominates elsewhere. Since the garnets are formed along fractures in clinopyroxene skarn, the formation and distribution of the amphiboles are thought to be controlled by the fracture system.

Cummingtonite–grunerite is not common in skarn-type ore deposits. It has been reported only from the Obira and Mitate mines in Japan (Miyahisa 1958, Kato 1973). The cummingtonite–grunerite from the Kamaishi mine is colorless to pale green under the microscope and generally fibrous (Fig. 3B). Recrystallized idiomorphic cummingtonite–grunerite is observed in certain samples (Fig. 3C). Calcite, quartz and a small amount of idiomorphic magnetite fill the interstices of the cummingtonite–grunerite. These minerals are all considered to be formed during amphibolitization of clinopyroxene. Cummingtonite–grunerite is accompanied by a variable amount of Ca-amphibole. Cummingtonite – grunerite rimmed with Ca-amphibole is sometimes observed (Fig. 4A). Thus the cummingtonite – grunerite may have been replaced by Ca-amphibole at a late stage.

Ca-amphibole is generally idiomorphic to hypidiomorphic and may contain relics of clinopyroxene (Fig. 3D), whereas no relics of clinopyroxene are observed in cummingtonite–grunerite. The color of the Ca-amphibole varies from colorless to dark green according to its Al content. Ca-amphibole is accompanied by small amounts of calcite, quartz and magnetite. Though it is not easy to distinguish actinolite from hornblende in some cases, there is a tendency for hornblende to dominate where garnet networks occur. The amount of actinolite increases with distance from the networks. Actinolite rimmed with hornblende is sometimes observed, which may indicate the replacement of actinolite by later hornblende (Fig. 5, Table 1). Figure 6 shows schematically the distribution of amphiboles in the exoskarns (clinopyroxene skarn and garnet skarn).

A large amount of Ca-amphibole occurs in the iron–copper orebody. The grains are idiomorphic to hypidiomorphic. They are either alteration products of clinopyroxene or primary products. They coexist with magnetite, chalcopyrite, pyrrhotite, pyrite, calcite, quartz, epidote and anisotropic garnet.

The amphibole in the epidote–amphibole and plagioclase–amphibole skarns is considered to have been derived from the original rocks, diorite to diorite porphyry. It consists of coarse and idiomorphic to hypidiomorphic grains of Ca-amphibole, generally forming twinned crystals.

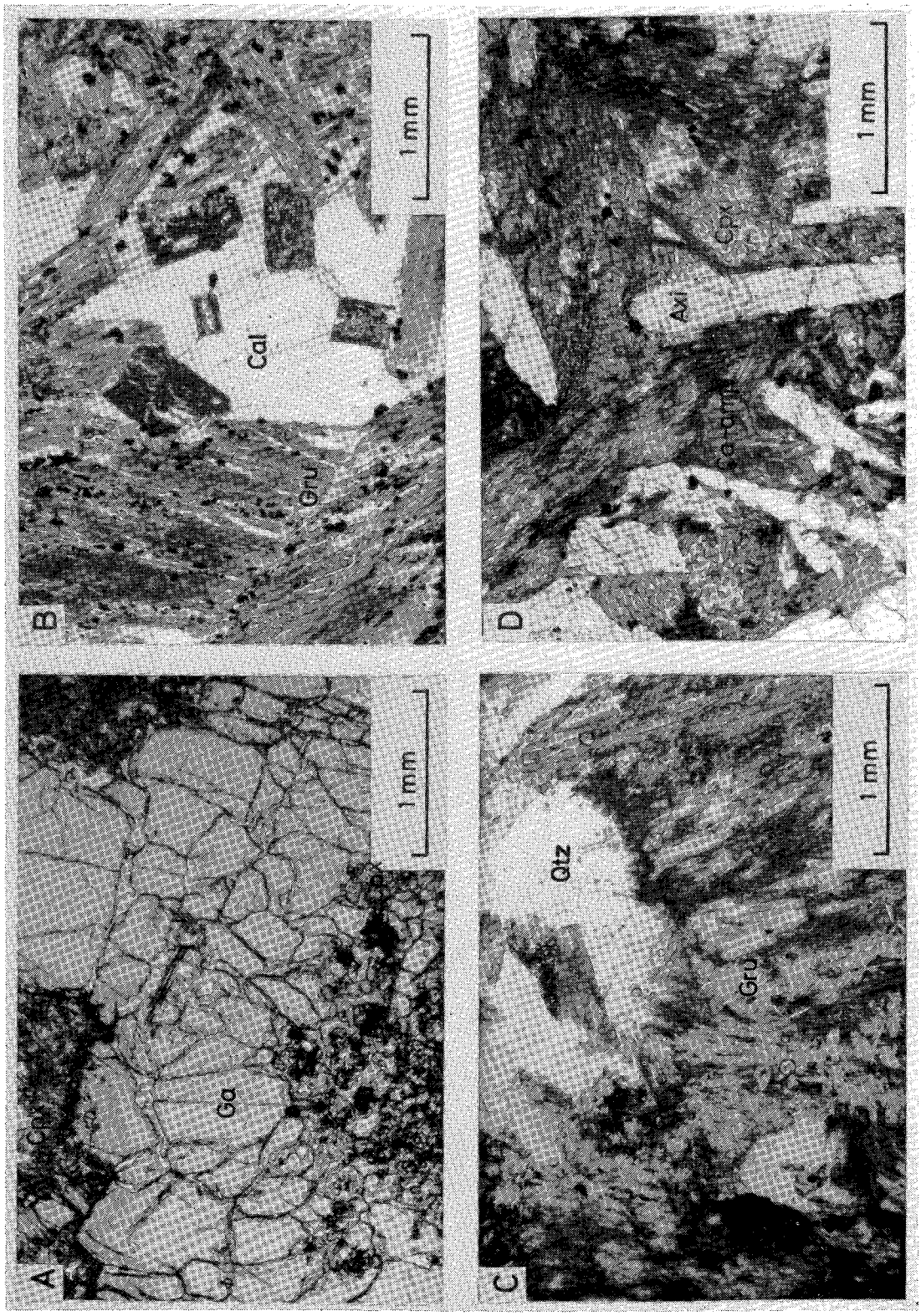
A
Ga
Cal
1 mm
B
Cal
Gru
1 mm
C
Qtz
Gru
1 mm
D
Axi
Cpx
Ca-amph
1 mm

Chemical Composition of the Amphiboles and Skarns

The amphiboles

The amphiboles in the clinopyroxene skarn were analyzed by the electron-probe microanalyzer. Chemical compositions are listed in Table 1. Cummingtonite–grunerite contains only about 1 wt.% CaO.

Figure 7 shows the relation between (Na + K) and ^{iv}Al (molar basis) in the Ca-amphibole. The Ca-amphibole in the clinopyroxene skarn shows a wide variation of (Na + K) and ^{iv}Al contents, perhaps because some grains of actinolite were altered to late hornblende as referred to above.

The Mg/(Mg + Fe) mole fractions of Ca-amphibole and cummingtonite–grunerite range from 0.24 to 0.38 and from 0.27 to 0.33, respectively. Amphibole compositions of the cummingtonite–grunerite series can be divided according to the Mg/(Mg + Fe) mole fraction (Leake 1978) into cummingtonite [X(Mg) > 0.3] and grunerite [X(Mg) < 0.3]. However, the amphibole of the cummingtonite–grunerite series in the clinopyroxene skarn is called grunerite for convenience.

The skarns

The chemical analyses were carried out on representative samples of limestone, clinopyroxene skarn and garnet skarn (analyst: H. Haramura). The results are shown in Table 2 (*cf.* Figs. 14, 15 in Uchida & Iiyama 1982). The results show that the CaO content in these rocks is nearly constant. The zonal arrangement in exoskarns thus cannot be attributed to the gradient of the chemical potential of CaO. On the other hand, the Al_2O_3 content increases gradually toward the garnet-skarn side. Therefore, it may be possible to consider that the zonal arrangement in exoskarns is attributable to a gradient in the chemical potential of Al_2O_3 (Uchida & Iiyama 1982).

Thermochemical Considerations of the Stability Relations among Minerals in Clinopyroxene Skarn

Considerations of temperature and CO_2 mole fraction in the fluid phase, $X(CO_2)$

The mineral assemblages are grunerite + calcite +

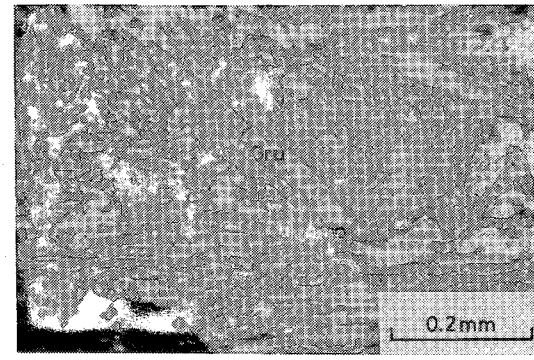

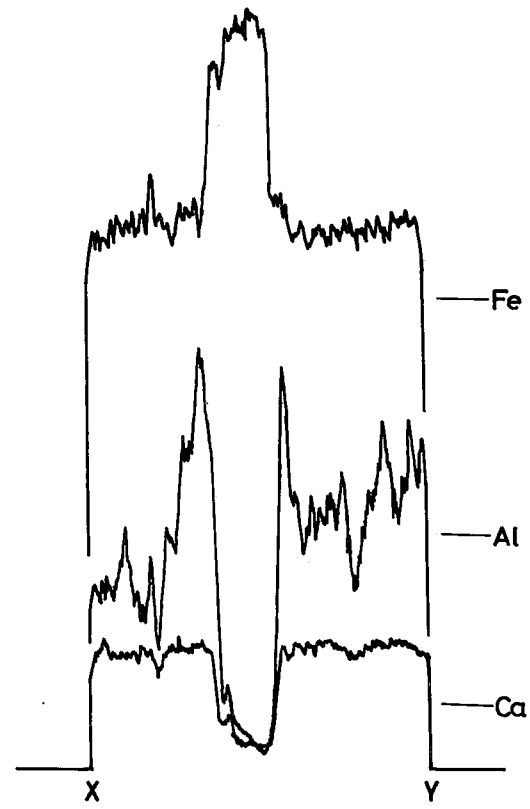

FIG. 4. A. Photomicrograph of cummingtonite–grunerite (Gru) rimmed with Ca-amphibole (Ca-amp). Sample number 307. B. Scanning profile of grunerite rimmed with Ca-amphibole along the line X–Y in A by the electron-probe microanalyzer.

FIG. 3. A. Photomicrograph of network garnet (Ga) in clinopyroxene skarn of the Shinyama 4D–7D orebodies. Sample number 404. B. Photomicrograph showing the replacement texture in which fibrous cummingtonite–grunerite (Gru), calcite (Cal), quartz and magnetite have replaced clinopyroxene. Sample number 303. C. Photomicrograph of recrystallized cummingtonite–grunerite in fibrous cummingtonite–grunerite. Sample number 2403. Qtz: quartz. D. Photomicrograph showing the relics of clinopyroxene (Cpx) in Ca-amphibole (Ca-amp). Sample number 408. Axi: axinite.

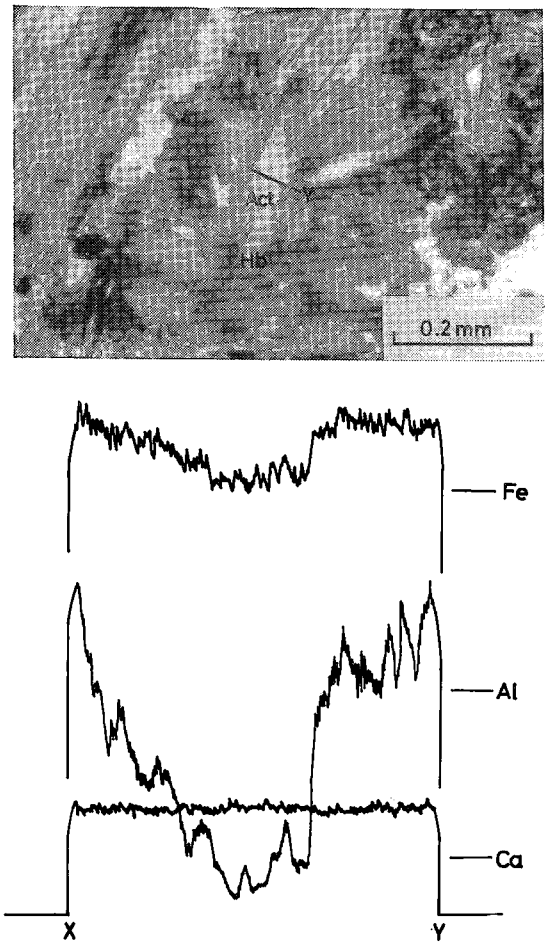

FIG. 5. A. Photomicrograph of actinolite (Act) rimmed with hornblende (Hb). Sample number 403. B. Scanning profile of actinolite rimmed with hornblende along the line X–Y in A by the electron-probe microanalyzer.

quartz, and Ca-amphibole + calcite + quartz; it is presumed that they formed through the following reactions, respectively:

$$7Hd + H_2O + 7CO_2 = Gru + 7Cal + 6Qtz \quad (1)$$
$$5Hd + H_2O + 3CO_2 = Act + 3Cal + 2Qtz \quad (2)$$

Since relics of clinopyroxene are commonly observed in Ca-amphibole, it is probable that the formation of Ca-amphibole generally obeys reaction (2). On the other hand, it is not proven that grunerite formed through reaction (1), no relics of clinopyroxene having been observed in grunerite. Grunerite may also have formed from Ca-amphibole through the following reaction:

$$7Act + 14CO_2 = 5Gru + 14Cal + 16Qtz + H_2O \quad (3)$$

Therefore, it is possible that grunerite formed indirectly from clinopyroxene through reactions (2) and (3). Two other reactions exist among clinopyroxene, Ca-amphibole, grunerite, calcite and quartz:

$$3Act + 2Cal = Gru + 8Hd + 2H_2O \quad (4)$$
$$7Act = 3Gru + 14Hd + 4\,Qtz + 4H_2O \quad (5)$$

Univariant equilibrium curves for the above reactions under a constant total pressure of one kbar were calculated thermochemically. The data for minerals (Table 3) were taken mainly from Helgeson *et al.* (1978). Owing to a lack of thermochemical data, Ca-amphibole is treated here as actinolite. Fugacity data for H_2O and CO_2 are taken from Burnham *et al.* (1969) and Majumdar & Roy (1956), respectively. Calculations were carried out on the following assumptions: i) fluid pressure, $P(H_2O) + P(CO_2)$, is equal to the total pressure; ii) constant volume change of reaction for minerals; iii) ideal mixing between H_2O and CO_2, and iv) independency of heat capacity on pressure.

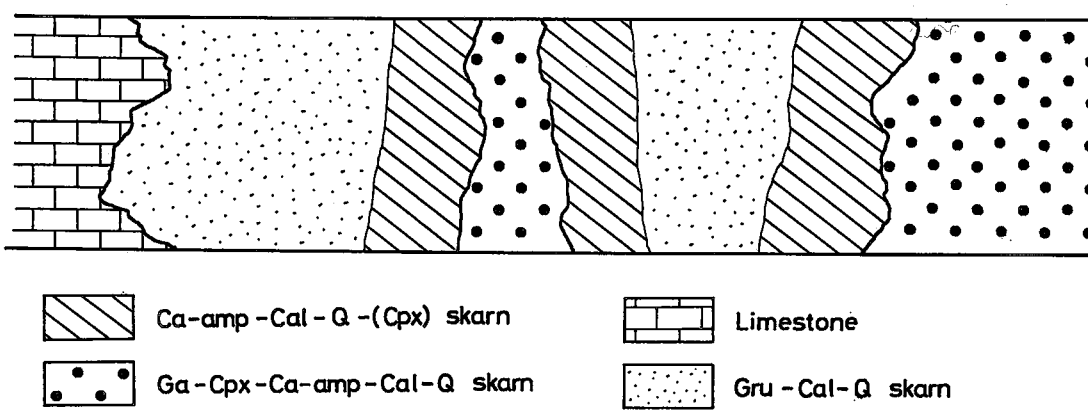

FIG. 6. Schematic sketch showing the distribution of amphiboles in clinopyroxene skarn.

TABLE 1. CHEMICAL COMPOSITION OF AMPHIBOLE SPECIES IN THE CLINOPYROXENE SKARN

	Grunerite		Actinolite		Hornblende	
Sample	303	307	403	2407	403	408
SiO_2	49.88	49.89	50.36	51.11	45.00	46.00
Al_2O_3	0.20	0.23	1.67	0.68	7.02	5.16
TiO_2	0.03	0.00	0.02	0.00	0.13	0.07
FeO*	35.75	34.93	23.59	23.89	25.26	25.15
MnO	1.82	1.92	1.06	1.24	0.98	1.01
MgO	7.38	8.39	7.85	7.54	5.09	6.02
CaO	1.47	0.68	11.84	11.55	11.37	11.78
Na_2O	0.08	0.04	0.09	0.05	0.51	0.35
K_2O	0.02	0.01	0.03	0.02	0.37	0.32
Total	96.63	96.09	96.51	96.08	95.73	95.86
Numbers of cations on the basis of 23 oxygen atoms						
Si	7.95	7.95	7.78	7.87	7.14	7.28
Al^{iv}	0.04	0.04	0.22	0.12	0.86	0.72
Al^{vi}	0.00	0.00	0.09	0.00	0.45	0.25
Ti	0.00	0.00	0.00	0.00	0.02	0.01
Fe^{2+}	4.77	4.66	3.05	3.08	3.35	3.33
Mn	0.25	0.26	0.14	0.16	0.13	0.13
Mg	1.75	1.99	1.81	1.73	1.20	1.42
Ca	0.25	0.11	1.96	1.91	1.93	2.00
Na	0.02	0.01	0.03	0.01	0.16	0.11
K	0.00	0.00	0.01	0.00	0.07	0.07

* Total Fe as FeO

Calculation in the Fe end-member system

As thermochemical data for grunerite and actinolite are not tabulated in Helgeson *et al.* (1978), they were obtained by the method described below.

Standard entropy and molar volume of grunerite were taken from Mel'nik (1972) and heat capacity from Miyano (1976). Standard enthalpy of formation was compiled from experimental results on grunerite coexisting with magnetite, pyrrhotite and quartz (Popp *et al.* 1977). From the experimental results of Popp *et al.* (1977), Froese (1977) obtained $\Delta G^\circ + \Delta V^\circ_{solid}(P - 1) = -102$ kcal/mol at 700°C and 1 kbar for the following reaction:

$$Gru + \frac{7}{6} O_2 = \frac{7}{3} Mag + 8Qtz + H_2O \qquad (6)$$

The standard enthalpy of formation ($\Delta H^\circ_{f,298}$) for grunerite is estimated from the data mentioned above to be -2286 kcal/mol. On the other hand, Mel'nik (1972) showed $\Delta H^\circ_{f,298}$(grunerite) to be -2294 kcal/mol.

The molar volume of actinolite was taken from Helgeson *et al.* (1978), and its heat capacity was evaluated from the data on heat capacities for tremolite, anthophyllite and grunerite. Standard enthalpy of formation $\Delta H^\circ_{f,298}$ and standard entropy S°_{298} were estimated to be -2501.8 kcal/mole and 176 cal/deg.mol, respectively, from the experimental equilibrium curve for the reaction

$$2Act = 3Fa + 5Qtz + 4Hd + 2H_2O \qquad (7)$$

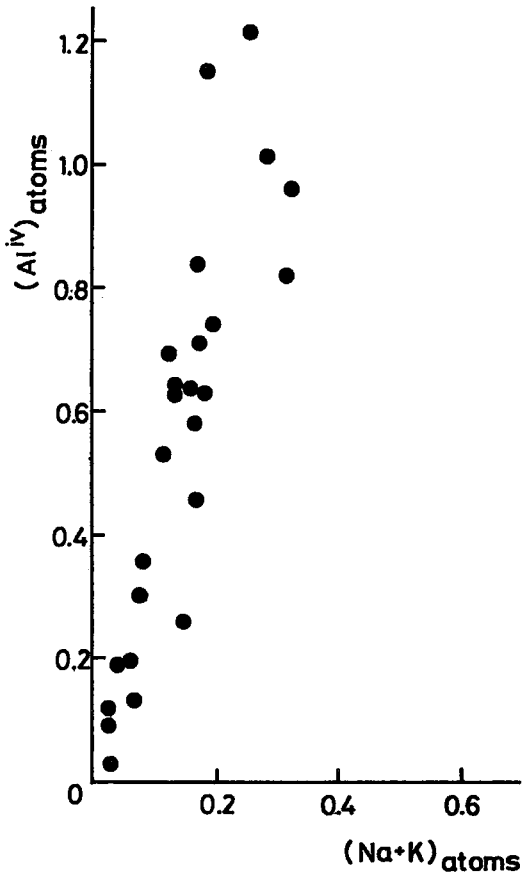

FIG. 7. Relation of (Na + K) and ^{iv}Al content of the Ca-amphibole in clinopyroxene skarn.

TABLE 2. CHEMICAL COMPOSITION OF LIMESTONE AND SKARNS

Sample	301	303	304	407	404	408
Rock	Ls	Cpx	Cpx	Cpx	Ga	Ga
SiO_2	0.13	37.59	28.88	39.77	41.33	37.81
TiO_2	trace	0.04	0.08	0.15	0.26	0.24
Al_2O_3	trace	0.56	0.85	2.60	5.60	8.15
Fe_2O_3	trace	6.75	5.07	6.37	7.49	6.84
FeO	0.07	14.03	13.88	10.39	12.08	7.59
MnO	0.01	0.81	1.00	0.74	0.86	0.78
MgO	0.47	2.70	3.27	2.31	2.56	2.23
CaO	56.11	19.58	26.23	23.24	25.47	26.44
Na_2O	0.02	0.05	0.08	0.12	0.17	0.13
K_2O	0.02	0.18	0.06	0.13	0.12	0.17
P_2O_5	0.02	0.02	0.07	0.07	0.08	0.16
Ig. loss	43.67	17.98	19.50	13.74	4.02	8.85
Total	100.52	100.29	98.97	99.63	100.04	99.39

Analyst: H. Haramura. Mineral assemblages: 301 Cal, 303 Gru, Cal, Qtz and Ca-amp, 304 Gru, Cal, Qtz and Ca-amp, 407 Gru, Ca-amp, Cal and Qtz, 404 Ga, Cpx, Ca-amp, Cal and Qtz, 408 Ga, Cpx, Ca-amp, Cal and Qtz.

as determined by Ernst (1966).

Calculated univariant curves at 1 kbar for reactions (1) to (5) are shown in Figure 8. The invariant

TABLE 3. THERMOCHEMICAL DATA FOR MINERALS AND GASES

	$\Delta H^\circ_{f,298}$ (kcal/mol)		S°_{298} (cal/deg.mol)		V°_{298} (cc/mol)		Cp° (cal/deg.mol) a	$b\times10^3$	$-c\times10^{-5}$	
Actinolite	-2501.8	a	176	a	282.8		189.056	72.38	36.128	a
Andradite	-1381.005		70.13		131.85		113.532	15.636	30.889	
Anthophyllite	-2888.749		128.6		264.4		180.682	60.574	38.462	
Calcite	-288.772		22.15		36.934		24.98	5.24	6.20	
Diopside	-765.598		34.2		66.09		52.87	7.84	15.74	
Grunerite	-2286.0	a	187.0	b	278.116	b	181.85	81.7	26.29	c
Fayalite	-354.119		35.45		46.39		36.51	9.36	6.7	
Hedenbergite	-678.496		40.7		68.27		54.81	8.17	15.01	
Hematite	-197.720		20.94		30.274		23.49	18.60	3.55	
Iron(α)	0	d	6.52	d	7.092	d	3.04	7.58	-0.60	e
Magnetite	-267.250		34.83		44.524		21.88	48.20	0.00	
Pyrite	-41.000		12.65		23.940		17.88	1.32	0.0	
Pyrrhotite(FeS)	-24.000		14.41		18.20		5.19	26.40	0.0	
Quartz(α)	-217.650		9.88		22.688		11.22	8.20	2.70	
Talc	-1410.920		62.34		136.25		82.48	41.61	13.34	
Tremolite	-2944.478		131.19		272.92		188.222	57.294	44.822	
H_2O(gas)	-57.796	d	45.104	d			7.300	2.46	0.0	e
CO_2(gas)	-94.051	d	51.060	d			10.570	2.10	2.06	e
O_2(gas)	0		49.003				7.16	1.0	0.4	
S_2(gas)	30.680		54.51				8.72	0.16	0.90	

References: a this study, b Mel'nik (1972), c Miyano (1976), d Robie & Waldbaum (1968), e Kelley (1960); all other entries: Helgeson *et al.* (1978). $Cp^\circ = a + bT + cT^{-2}$.

point (Hd, Act, Gru, Cal and Qtz) for these five univariant curves is located at 475°C and $X(CO_2) = 0.17$ at 1 kbar. Reaction (1) is stable under high temperature and $X(CO_2)$ conditions in comparison with the invariant point, and reactions (2) and (3) are stable under low temperature and $X(CO_2)$ conditions. The value for the standard enthalpy of formation for grunerite has an associated error of at least ±1 kcal/mol. With this error, the invariant point shifts from 430°C and $X(CO_2) = 0.08$ with $\Delta H^\circ_{f,298} = -2287$ kcal/mol to 505°C and $X(CO_2) = 0.35$ with $\Delta H^\circ_{f,298} = -2285$ kcal/mol.

Calculation in the Mg end-member system

Owing to a lack of thermochemical data for cummingtonite, the phase relations among diopside, tremolite, anthophyllite, calcite and quartz are discussed here. Calculated univariant curves for equivalent reactions to reactions (1) to (5) are shown in Figure 9. The invariant point (Di, Tr, Ant, Cal and Qtz) in this system is located at 410°C and $X(CO_2) > 0.99$. The univariant assemblage of reaction (1)′ is stable in the extremely high $X(CO_2)$ region and that of reaction (3)′ is also stable in the relatively high $X(CO_2)$ or low temperature region. Therefore, the formation of anthophyllite through reaction (1)′ or (3)′ cannot be expected in skarn-type ore deposits. In fact, reactions (1)′ and (3)′ are not stable because anthophyllite is stable only in the hatched region of Figure 9 (Johannes 1969). The following reaction is stable in the low $X(CO_2)$ region.

$$3Tr + 2H_2O + 6CO_2 = 6Cal + 4Qtz + Tc \quad (8)$$

Talc instead of anthophyllite thus is formed by the decomposition of tremolite. Talc formed by such alteration is observed in the Akatani and Sennin mines (Imai 1960).

Discussion

The invariant point for the Fe end-member system is located in the low $X(CO_2)$ region, and that for the Mg end-member system at high $X(CO_2)$. Since the Fe/(Fe + Mg) mole fractions of clinopyroxene, Ca-amphibole and grunerite in clinopyroxene skarn are about 0.7, the invariant point for the five naturally occurring mineral phases (Tr–Act, Cumm–Gru, Di–Hd, Cal and Qtz) must be located in a higher $X(CO_2)$ region than the invariant point for the Fe end-member system. If the temperature gradient could be neglected, the distribution of clinopyroxene and amphiboles in the clinopyroxene skarn can be explained by the gradient of $X(CO_2)$ based on the calculated phase-relations. Clinopyroxene is stable in the lower $X(CO_2)$ region below the temperature of the invariant point of Figure 8. With an increase of $X(CO_2)$, clinopyroxene decomposes at first to actinolite + quartz + calcite [reaction (2)], and then actinolite to grunerite + quartz + calcite [reaction (3)]. As described in the previous chapter,

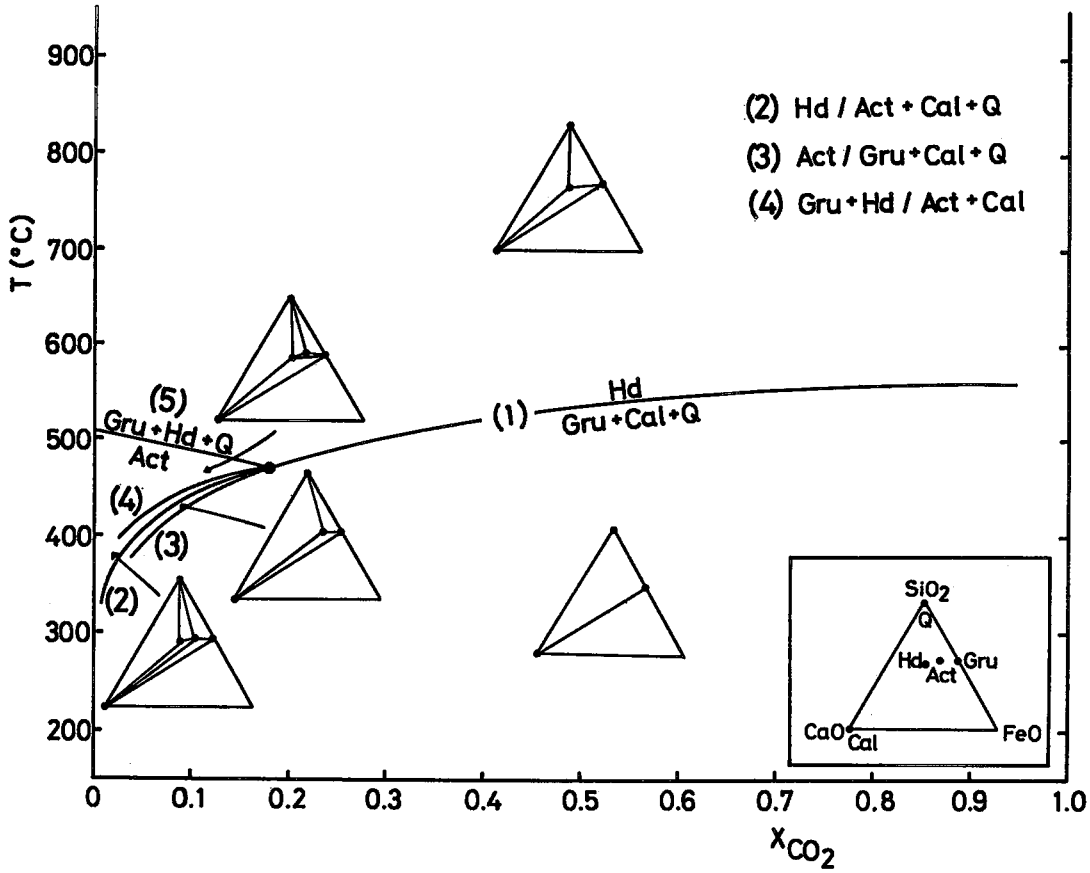

FIG. 8. Calculated univariant curves among hedenbergite (Hd), actinolite (Act), grunerite (Gru), calcite (Cal) and quartz (Q). Total pressure is 1 kbar.

Ca-amphibole and clinopyroxene occur where fracture systems are developed, and grunerite elsewhere. CO_2 released by skarn formation could escape along fractures. Therefore, where fractures are developed, $X(CO_2)$ may have been relatively lowered, and Ca-amphibole, instead of grunerite, could form by the alteration of clinopyroxene.

There are two ways to explain the amphibolitization of clinopyroxene. One is an increase of $X(CO_2)$ at constant temperature, and the other is a decrease of temperature. Since CO_2 is probably generated by the decomposition of calcite, it is reasonable in the former case to expect that amphibole can be formed primarily instead of clinopyroxene at the front of skarn formation; clinopyroxene could then replace the amphiboles later owing to a decrease of $X(CO_2)$ [reaction (1) or (2)]. As described above, this is not seen in the deposit studied. Amphibole replaces clinopyroxene in the clinopyroxene skarn. Therefore, a decrease of the temperature is considered to be a main factor for amphibolitization of clinopyroxene.

Thus, it is considered that grunerite was formed under relatively high $X(CO_2)$ conditions. As described before, no relics of clinopyroxene are observed in grunerite. This fact can be explained by proposing that clinopyroxene decomposed more easily in the grunerite skarn because the mineral assemblage grunerite + calcite + quartz is stable at a higher $X(CO_2)$ condition than the mineral assemblage actinolite + calcite + quartz. Also, grunerite is formed only at the 4D orebody in the Kamaishi mine. This fact can be explained by proposing that CO_2 could escape easily in the other orebodies compared to the situation in the 4D orebody. In other words, the occurrence of grunerite is considered to be structurally controlled.

Conditions of $f(O_2)$ and $f(S_2)$

The following reactions may occur between grunerite and Fe–S–O minerals (Froese 1977):

$$2\text{Gru} = 14\text{Fe} + 16\text{Qtz} + 2H_2O + O_2 \qquad (9)$$

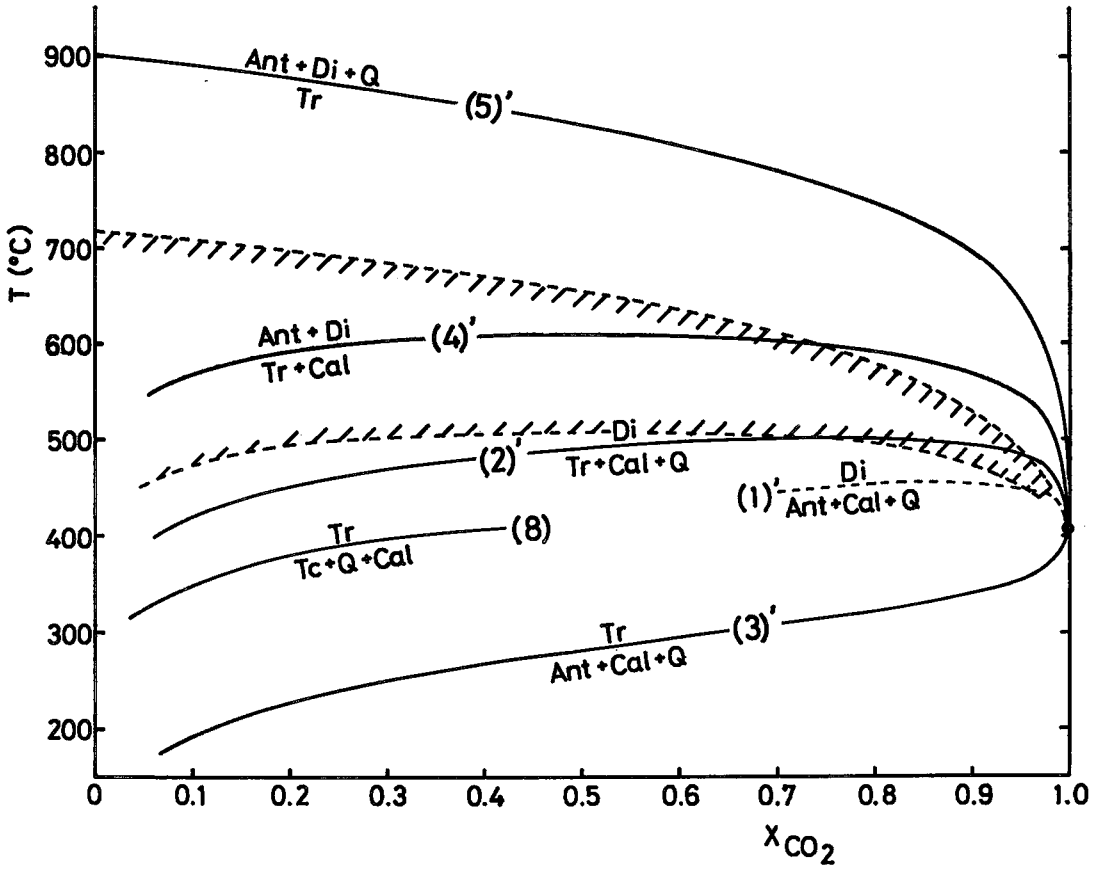

FIG. 9. Calculated univariant curves among diopside (Di), tremolite (Tr), anthophyllite (Ant), calcite (Cal) and quartz (Q). Total pressure is 1 kbar. The stability region of anthophyllite is surrounded by hatched lines. Abbreviations: Tc, talc.

$$6Gru + 7O_2 = 14\,Mag + 48Qtz + 6H_2O \quad (10)$$
$$4Gru + 7O_2 = 7Hm + 32Qtz + 4H_2O \quad (11)$$
$$2Gru + 7S_2 = 14Po(FeS) + 16Qtz + 2H_2O + 7O_2 \quad (12)$$
$$2Gru + 14S_2 = 14Py + 16Qtz + 2H_2O + 7O_2 \quad (13)$$

Figure 10 shows the calculated phase-diagram at 400°C and 1 kbar. The amphibole of the cummingtonite–grunerite series was assumed to be an ideal solid-solution in this calculation. Thermochemical data for minerals in the system Fe–S–O (Table 3), except for iron, were taken from Helgeson *et al.* (1978). Thermochemical data for iron were taken from Robie & Waldbaum (1968) except for the heat capacity (Kelley 1960).

Grunerite in clinopyroxene skarn coexists not only with calcite and quartz, but also with magnetite. As the Fe/(Fe + Mg) mole fraction of grunerite is also about 0.7 in the orebody studied, the log $f(O_2)$ is estimated to be about -27.8 for these mineral assemblages at 400°C and 1 kbar. Grunerite also exists with pyrrhotite. This fact is consistent with calculated results. The log $f(S_2)$ is estimated to be about -9.0 at 400°C and 1 kbar for the mineral assemblage of magnetite, pyrrhotite, quartz and grunerite with a Fe/(Fe + Mg) mole fraction of 0.7.

STABILITY RELATIONS AMONG THE MINERALS IN EXOSKARNS

Two kinds of exoskarns are observed in the vicinity of the Shinyama 4D orebody. One is clinopyroxene skarn composed of grunerite, Ca-amphibole, calcite, quartz and clinopyroxene. The other is garnet skarn composed of garnet, clinopyroxene, Ca-amphibole, calcite and quartz. The zonal arrangement observed in the exoskarns at present is as follows from the limestone side to garnet skarn: limestone, grunerite skarn, Ca-amphibole skarn, (clinopyroxene skarn) and garnet skarn. It was shown above that the

distribution of amphibole and clinopyroxene in the clinopyroxene skarn can be explained by the existence of a gradient in $X(CO_2)$. The phase equilibria in the system CaO–Fe–SiO_2–H_2O–CO_2–O_2 were calculated in order to examine whether this idea is applicable even for the distribution of garnet. Thermochemical data for andradite were taken from Helgeson *et al.* (1978). Figure 11 shows the calculated position of the principal univariant curves at 420°C and 1 kbar. (This diagram is complicated below 400°C.) Andradite is stable in the relatively low $X(CO_2)$ region below log $f(O_2)$ = -27.6. With an increase of $X(CO_2)$, andradite decomposes to hedenbergite + calcite + magnetite, hedenbergite to actinolite + calcite + quartz, and actinolite to grunerite + calcite + quartz. From these results, the following zonal arrangement can be expected with an increase of $X(CO_2)$: andradite skarn, hedenbergite skarn, actinolite skarn, and grunerite skarn. Therefore, the zonal arrangement in exoskarns is attributed to the gradient of $X(CO_2)$; $X(CO_2)$ is considered to decrease from the limestone toward the garnet skarn.

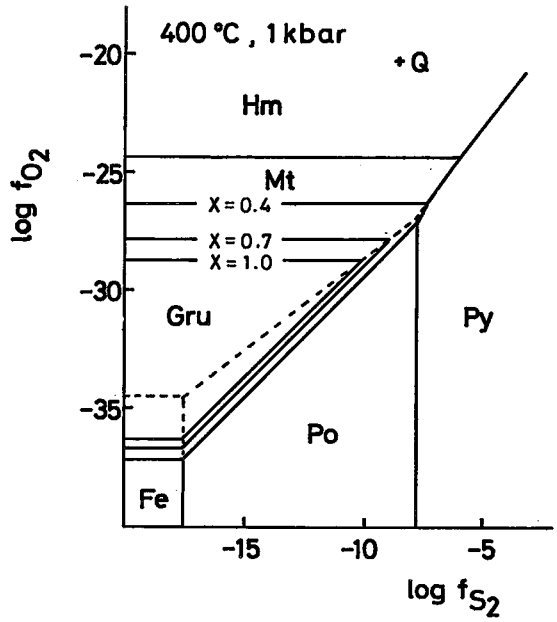

FIG. 10. Log $f(O_2)$ - log $f(S_2)$ diagram showing stability relations among grunerite and Fe–S–O minerals at 400°C and 1 kbar. SiO_2 is an excess component. X indicates the mole fraction of grunerite molecule in the cummingtonite–grunerite series amphibole. Abbreviations: Gru grunerite, Q quartz, Hm hematite, Mt magnetite, Po pyrrhotite(troilite), Py pyrite.

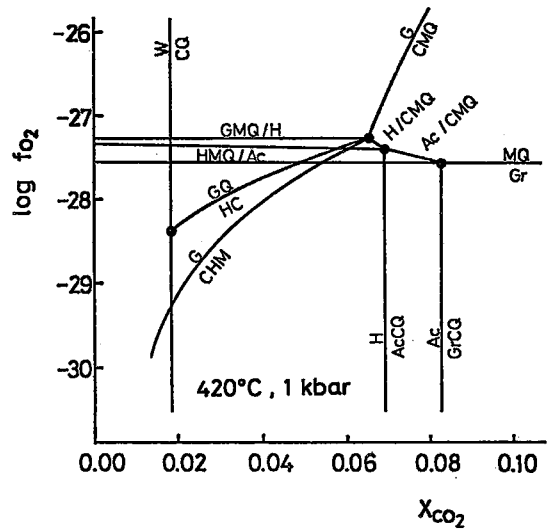

FIG. 11. Log $f(O_2)$ - $X(CO_2)$ diagram in the system CaO–Fe–SiO_2–H_2O–CO_2–O_2 at 420°C and 1 kbar. Only the principal univariant curves are shown in this diagram. Abbreviations: Ac actinolite, Gr grunerite, G andradite, C calcite, M magnetite, Q quartz, H hedenbergite.

CONCLUSIONS

Most of the clinopyroxene in the clinopyroxene skarn containing the 4D orebody was altered to grunerite and Ca-amphibole at a later stage. Amphibolitization of clinopyroxene is considered to have been caused by a decrease in temperature. The distribution of these minerals is controlled by the difference in the partial pressure of CO_2. Grunerite is formed under a relatively high $X(CO_2)$ condition and Ca-amphibole under a lower $X(CO_2)$ condition. Andradite is also stable under a relatively low $X(CO_2)$ condition. Therefore, the zonal arrangement observed at present in exoskarns, limestone, grunerite skarn, Ca-amphibole skarn, (clinopyroxene skarn), and garnet skarn, can be attributed to the increase of chemical potential of CO_2 toward the limestone. This zonal arrangement may also be promoted by the increase in the chemical potential of Al_2O_3 toward the garnet skarn.

ACKNOWLEDGEMENTS

I express my gratitude to Professor J.T. Iiyama and Dr. H. Shimazaki of the University of Tokyo for their helpful advice and critical reading of the manuscript. This work would have been impossible without the co-operation of the mining geologists of the Kamaishi Mining Company, Ltd. I am indebted to Mr. Haramura of the University of Tokyo for the wet chemical analyses. The two referees contributed very helpful comments.

REFERENCES

BURNHAM, C.W., HOLLOWAY, J.R. & DAVIS, N.F. (1969): Thermodynamic properties of water to 1,000°C and 10,000 bars. *Geol. Soc. Amer. Spec. Pap.* **132.**

ERNST, W.G. (1966): Synthesis and stability relations of ferrotremolite. *Amer. J. Sci.* **264,** 37-65.

FROESE, E. (1977): Oxidation and sulphidation reactions. *In* Application of Thermodynamics to Petrology and Ore Deposits (H.J. Greenwood, ed.). *Mineral. Assoc. Can., Short Course Handbook* **2,** 84-97.

HAMABE, S. & YANO, T. (1976): Geographical structure of the Kamaishi mining district, Iwate Prefecture, Japan. *Kozan Chishitsu (Mining Geol.)* **26,** 93-104 (in Japanese).

HELGESON, H.C., DELANY, J.M., NESBITT, H.W. & BIRD, D.K. (1978): Summary and critique of the thermodynamic properties of rock-forming minerals. *Amer. J. Sci.* **278A.**

IMAI, N. (1960): Genesis of the hematite deposits in the Inner Zone of Northeastern Japan, with special reference to those of the Akatani and Sen-nin iron mines. *J. Fac. Sci., Niigata Univ.(Ser. II)* **3,** 205-256.

JOHANNES, W. (1969): An experimental investigation of the system MgO-SiO_2-H_2O-CO_2. *Amer. J .Sci.* **267,** 1083-1104.

KATO, A., ed. (1973): *Sakurai Mineral Collection.* Committee on the celebration of Dr. K. Sakurai's sixtieth birthday, Tokyo (in Japanese).

KELLEY, K.K. (1960): Contributions to the data on theoretical metallurgy. XIII. High-temperature heat-content, heat-capacity, and entropy data for the elements and inorganic compounds. *U.S. Bur. Mines Bull.* **584.**

LEAKE, B.E. (1978): Nomenclature of amphiboles. *Can. Mineral.* **16,** 501-520.

MAJUMDAR, A.J. & ROY, R. (1956): Fugacities and free energies of CO_2 at high pressures and temperatures. *Geochem. Cosmochim. Acta* **10,** 311-315.

MEL'NIK, YU. P. (1972): *Thermodynamic Constants for the Analysis of Conditions of Formation of Iron Ores.* Inst. Geochem. Phys. Minerals, Nauka Dumka, Kiev, Ukranian S.S.R. (in Russ).

MIYAHISA, M. (1958): Contact metasomatic lead-zinc ore deposits of the Obira mine, Oita Prefecture, Japan. II. *J. Mining Inst. Kyushu* **26,** 19-30 (in Japanese).

MIYANO, T. (1976): Physicochemical environments during burial metamorphism of the Dales Gorge Member, Hamersley Group, western Australia. *Kozan Chishitsu (Mining Geol.)* **26,** 311-325 (in Japanese).

MUELLER, R.F. (1960): Compositional characteristics and equilibrium relations in mineral assemblages of a metamorphosed iron formation. *Amer. J. Sci.* **258,** 449-497.

POPP, R.K., GILBERT, M.C. & CRAIG, J.R. (1977): Stability of Fe-Mg amphiboles with respect to sulfur fugacity. *Amer. Mineral.* **62,** 13-30.

ROBIE, R.A. & WALDBAUM, D.R. (1968): Thermodynamic properties of minerals and related substances at 298.15 K (25.0°C) and one atmosphere (1.013 bars) pressure and at higher temperatures. *U.S. Geol. Surv. Bull.* **1259.**

UCHIDA, E. & IIYAMA, J.T. (1982): Physicochemical study of skarn formation in the Shinyama iron-copper ore deposit of the Kamaishi mine, Northeastern Japan. *Econ. Geol.* **77,** 809-822.

Received June 18, 1982, revised manuscript accepted October 30, 1982.